

Optical Continuum Variability of the Active Galaxy Mrk 279 – Implications for Different Accretion Regimes

R.BACHEV^{1,2} and A.STRIGACHEV¹

¹ Institute of Astronomy, Bulgarian Academy of Sciences, 72 Tsarigradsko Chausse Blvd., 1784 Sofia, Bulgaria

² Department of Physics and Astronomy, University of Alabama, Tuscaloosa, AL 35487, USA

Received *date will be inserted by the editor*; accepted *date will be inserted by the editor*

Abstract. We present results from a recent broad-band monitoring in optics of the Seyfert 1 type galaxy Mrk 279. We build and analyse the *BVRI* light curve covering a period of seven years (1995 – 2002). We also show some evidence for the existence of two different states in brightness and suggest, based on a modelling of the optical continuum, that these states may result from transition between a thin disk and an *ADAF* accretion modes. We assume that the short-term variability is due to a reprocessing of a variable X-ray emission from an inner *ADAF* part of the flow, while the long-term one may be a result from a change of the transition radius. Our tests show a good match with the observations for a reasonable set of accretion parameters, close to the expected ones for Mrk 279

Key words: galaxies: active – galaxies: Seyfert – galaxies: individual (Mrk 279) – galaxies: photometry

1. Introduction

The continuum variability is a well-known feature of many Active Galactic Nuclei (AGNs). It is usually thought that the variability of radio-quiet AGNs is connected to instabilities of the accretion flow, feeding the central supermassive black hole, unlike the case of blazars where similar variations are usually attributed to processes in a relativistic jet (Ulrich et al. 1997; Kawaguchi & Mineshige 1999). Therefore any knowledge about the continuum variations might shed some light onto the accretion process and respectively – the nature of the central engine of the active nuclei. Although many Seyfert galaxies are known to be variable, the variability of only a few of them has been studied intensively so far, which is our motivation to begin a program (Bachev et al. 2000) for optical monitoring of selected objects.

In this paper we present the results of a broadband *B*, *V*, *R_c* and *I_c* monitoring of the radio-quiet active galaxy Mrk 279. Mrk 279 is a relatively bright $V \approx 14^m$ spiral (*S0*), Seyfert 1 type galaxy, for which both continuum and emission-line profiles are known to vary in time (Stirpe 1991; Santos-Lleo et al. 2001). Combining the results from the reverberation mapping, which give a broad line region (BLR) radius of about 12-17 light days (Maoz et al. 1990; Santos-Lleo et al. 2001), and the width of the broad emission

lines (about 6000 *km/s*), the mass of the central object can be inferred – $M_{BH} \approx 10^8 M_{\odot}$ (Ho 1998). This mass and the nuclear bolometric luminosity of about 10^{45} *erg/s* give a rough estimate of the accretion rate of 0.01-0.1, measured in Eddington units (see also Bian & Zhao 2003). Since later we will propose that most probably two different accretion modes (Advection Dominated Accretion Flow – *ADAF* – and a thin disk) operate in this object, we point out here that this rate is rather close to the critical accretion rate of the transition between an *ADAF* and a thin disk accretion regimes, which is in general assumed to be of the same order – 0.01-0.1 (Narayan et al. 1998).

This paper is organised as follows: observations and reductions are presented in Sect. 2; in Sect. 3 we present some evidence for different states in brightness; Sect. 4 compares different variability scenarios and shows the results of the continuum modelling, under the assumptions of a change of the accretion disk structure. Sect. 5 is the discussion and we present our conclusions in Sect. 6. The table containing the *BVR_cI_c* magnitudes of Mrk 279 is given in the Appendix.

2. Observations and reductions

The major part of the observations were performed with the 0.6-m telescope of the Observatory of Belogradchik, Bulgaria, equipped with SBIG ST-8 CCD camera and Johnson-Cousins *BVR_cI_c* filters (Bachev et al. 1999;

Bachev et al. 2000). A few data points (JD 2450000+: 2066.3, 2096.3, 2099.3) were obtained using the 1.3-m telescope of the Skinakas Observatory, University of Crete, Greece, equipped with a Photometrics CH 360 CCD camera.

The monitoring covered a period of five years (July 1997 – June 2002). Standard aperture photometry was performed in order to estimate the AGN magnitudes. Star *A* and star *C*, whose magnitudes and finding charts can be found in Bachev et al. 2000, were used as the main standard and as a check respectively. The *B*-band magnitude of the main standard, not published in the paper cited above, was additionally calibrated – $B = 13^m.08$.

BVR_cI_c magnitudes of Mrk 279 were measured in 66 observational epochs and are given in Table 1 (Appendix). The typical sampling interval was several days with the exception of a few larger gaps. For each observational point at least two CCD frames in each filter were taken, with a typical exposure time of 120 sec. During the observations the seeing was usually 2–3'', which presumably did not affect the aperture photometry, performed in a much larger diaphragm (16''). The standard errors of the differential photometry are typically below 0^m.02 (about 0^m.05 for *B*-band). The object showed significant variability during the observational period (Fig. 1) with time scales starting from 1 day. Short-term (1–4 hours) variations were searched extensively for more than a total of 20 hours in *V* and *I*-bands, but were not detected above the limit of the photometric errors.

We used, in addition, recently published results on monitoring of Mrk 279 in optics and near-IR (Santos-Lleo et al. 2001). Except spectroscopically, the object was also monitored in *BVRI* bands with the 1-m telescope of Wise Observatory using a 7'' diaphragm. Although not scaled to any photometric system, we were able to use these broad-band magnitudes for our purposes by fitting smooth curves to both data sequences and comparing these two fits in an overlapping observational epoch. Thus we obtained the following relations between our magnitudes and those from the Wise Observatory observations (Santos-Lleo et al. 2001):

$$\begin{aligned} B_{our} &= B_{Wise} + 0.50, \\ V_{our} &= V_{Wise} + 1.38, \\ R_{our} &= R_{Wise} + 0.91, \\ I_{our} &= I_{Wise} + 0.33, \end{aligned}$$

with a typical error of these transformations of about 0^m.03. After rescaling the Wise data we built a combined light curve, covering an observational period of about seven years (Fig. 1).

3. Evidence for different states in brightness

The *V*-band light curve of the monitored AGN is shown in Fig. 1. The variations in other bands occurred with no detectable time lags (less than 1 day), which, in addition to the rapid changes of brightness, restricts the dimension of the region producing the bulk of the variable part of the continuum to about 1 l.d. (or about 100 R_G in this case,

$R_G = 2GM_{BH}/c^2$). Using the obtained light curve, we find some arguments that the object shows signatures of two different states in brightness. These arguments can be summarised in the following way:

3.1. Magnitude histograms

The distribution of the magnitude points (over 80 in total) is most likely bimodal, with a clear gap at $V \approx 13^m.90$ where no observational points can be found (Fig. 2). Statistically, the presence of such a dip is quite unlikely if a *Gaussian* distribution of the sample is assumed. The *Gaussian* distribution hypothesis can be ruled out on the 95% probability level (at least for *R* and *I*-bands), as our analysis shows.

Surprisingly, the gap is best seen in *I*-band and is absent in *B*-band. This result cannot be attributed to the photometric errors only, which indeed increase toward shorter wavelengths. Most likely this gap indicates the presence of two types of variability: long-term (≈ 100 days) variations responsible for the transitions between the states, and short-term (1–10 days) variations. If so, the variability amplitudes must depend on the colour in different ways for the short and the long-term variability, producing the magnitude distribution picture shown.

3.2. Colour-magnitude diagram

There is a slight but well detectable jump in the colour-magnitude relation (Fig. 3) at the point where the transition between the states is expected, indicating that the physical processes, responsible for the continuum emission, probably change during that transition. Note that the magnitudes shown here (*V* and *I*) cover wavelength areas, which are generally located out of the places where strong (and presumably variable) emission lines are present, i.e. we observe and analyse only the continuum variability. In fact, a similar jump is observed for the other colours as well, but it becomes more evident with the increase of the wavelength difference. From a statistical point of view, the transition process should be relatively fast, based on the absence of magnitude points around the jump, while the adjacent areas are heavily populated (Fig. 3). Our interpretation is that this is possibly a manifestation of a two-state behaviour. Possible observational errors could hardly account for the jump (see Fig. 3 for details).

3.3. Structure Function

In order to find further arguments in favour of the two-state behaviour of Mrk 279, we invoke the first-order Structure Function - *SF* (di Clemente et al. 1996). This function is similar to the power density spectrum in some sense, but it is easier to build for an unevenly spaced data. For the AGN case, the *SF* is usually characterised by a saturation time τ_{var} , after which the *SF*, initially rising with a slope of 0.3–0.7 (Kawaguchi & Mineshige 1999; Collier & Peterson 2001), begins to turn over and remains nearly a constant. At timescales greater than the saturation time, τ_{var} , the amplitude of the variations does not increase,

indicating that τ_{var} is probably associated with some of the timescales of the physical processes driving the variability.

In order to search for differences in the nature of the short-term (1-10 days) and the long-term variability (≈ 100 days), we build SF 's separately for the lower and the higher state. These functions are based on 30 and 18 observational points respectively (Fig. 4) and cover the periods where the object has been most intensively monitored. Although there is a significant scatter, we see indications that the nature of the variability may really be different for these two states. In particular, the saturation time (τ_{var}) appears to be much shorter for the higher state (about 5 days) than for the lower state (about 20 days), Fig. 4.

4. Modelling the continuum variability

In this section we consider several schemes that can, in principle, account for the observed variability picture and elaborate the possibility that a change of the accretion disk structure is primarily responsible for the bimodal behaviour.

4.1. Accretion disk structure changes

We adopted a simple model to test the possibility of reproducing the observed variability. The accretion flow is assumed to consist of an inner advection part operating at $r < R_{tr}$ and an outer, thin-disk part at $R_{tr} < r < R_{out}$. The thin disk emits as a blackbody in optics. The inner optically thin ADAF is assumed not to contribute to the optical continuum itself, but its hard X-rays might irradiate the outer part, increasing the temperature and producing some extra optical flux there. Since the short-term variations occur on time-scales of about a day, we accept that they are produced by variations of the central X-ray emission, reprocessed by the outer parts in optics. The geometry of the central X-ray emitting region is taken, in our simple model, to be a uniform sphere with radius R_{tr} . In such a case, the bulk of the emission will come from a typical height $H_s = 4R_{tr}/3\pi$ above the disk. A more realistic geometry might be more relevant, but we believe it will not change the results much. As one can show, the absorbed X-ray flux at a given radial distance (F_x) is roughly proportional to the product of H_s and L_x , and we consider L_x as a free parameter anyway (see below). Furthermore, any specific geometry could hardly be justified, so we adopt the simplest case. Any flaring and possible warping of the disk were neglected. We assume that the switch between the states is due to a relatively fast change of the transition radius between two metastable positions (R_1 and R_2), which can occur for some critical accretion rate - \dot{m}_{cr} (see below).

We take R_{tr} , R_{out} , L_x , M_{BH} and \dot{m} to be free parameters (\dot{m} is the accretion rate expressed in Eddington units). We run a series of tests changing these parameters within some reasonable limits ($\log(M_{BH}) = 6 - 9$, $\dot{m} = 0.001 - 1$, $R_{tr} = 3 - 200R_G$). Our goal is to find a set of parameters that will reproduce our data well. To test our scheme we have to find out if the following will be fulfilled:

1. The adopted scheme could in principle reproduce the observed variability – time-scales, colour trends, jumps, etc. only by changing R_{tr} and L_x for given M_{BH} and \dot{m} .
2. The best working set of parameters found will be close to those already adopted for this object (see Sect. 1).
3. These parameters will be non-contradictory in between and consistent with the theoretical predictions.

In other words we try to find out if a non-contradictory accretion disk structure can account for the observed optical variability.

The effective temperature of the disk is $T(r) = T_G(r)[1 + F_x(r)/(\sigma T_G(r)^4)]^{1/4}$ K. This is the standard thin disk effective temperature, $T_G(r) = 3.5 \cdot 10^7 [\dot{m}/(\eta M_{BH} r^3)]^{1/4}$ K (Frank et al. 2002), corrected for the absorbed X-ray flux coming from the central ADAF. Here the radial distance r is expressed in R_G ; the accretion efficiency is taken $\eta = 0.1$. Thus, by assuming a blackbody radiation, we get for the overall emission at frequency ν to be $F_\nu \propto \int_{R_{tr}}^{R_{out}} B_\nu(r) r dr$; $B_\nu(r)$ is the Planck function. This flux can be consequently converted into magnitudes in order to be compared with the real observations.

Although one may think that there are many different sets of parameters that would be able to reproduce the observations equally well, the results from our tests indicate otherwise. For instance, to reproduce the overall colour-magnitude trend we had to restrict $\log(M_{BH}) > 7$ and $\dot{m} < 0.1$ for any reasonable R_{tr} ; otherwise, the slope turned out to be too steep, meaning an almost non-chromatic variability. We have to say that, in general, we failed to reproduce the colour jump in the way it was observed for any reasonable values of the parameters and $R_{out} = \infty$. The lower (corresponding presumably to a large R_{tr}) part of the colour-magnitude relation, appeared to be shifted to the red in respect to the upper part, which is exactly the opposite of what we see. We succeeded, however to get approximately the "right" jump pattern by reducing significantly R_{out} to 100 - 120 R_G . As we will see in the next section, such a low value for the outer boundary of the accretion disk is not entirely unrealistic from a theoretical point of view.

Fig. 5 shows two solutions for $\dot{m} = 0.01$ and $\log(M_{BH}) = 7.5$ and 8 respectively. The central X-ray flux L_x , responsible for the short-term variations, is still a free parameter, but is limited in a way that will not allow the absorbed (and re-emitted) flux to dominate in the total optical flux from the disk. The R_{tr} changes between $R_1 = 20R_G$ and $R_2 = 50R_G$ during the transition between the states. This choice is an empirical one, results from many tests, and provides a maximal separation between the states (see also Fig. 3), reaching nearly the observed one, without requiring unrealistically high R_2 . Other choices either would show no significant discontinuity in the colour-magnitude relation or a relatively much redder lower part, contrary to what was observed. Smaller values of R_1 seem to work somewhat worse but still acceptably well.

In other words we find that these two parameter sets (see above, also Fig. 5) reproduce the variability pattern best and are among the few that work at all.

Let us now see if the adopted set of parameters is physically relevant and intrinsically non-contradictory. First, one notices that the M_{BH} and \dot{m} values are indeed quite close to what we expected (Sect. 1). We also note that the saturation times (Sect. 3.3) are in very good agreement with the *Keplerian* times (or free-fall times) for about 20 and 50 R_G – respectively 4.5 and 18 days for $\log(M_{BH}) = 8$. The significance of this fact is discussed in the next section.

In addition, to be able to account for a transition between the states, the accretion rate has to be close to some critical value \dot{m}_{cr} , where an intermittent transition between the accretion modes would eventually occur. In fact, most theoretical approaches (Esin et al. 1997, Różanska & Czerny 2000) predict a discontinuous change of the transition radius for some certain (critical) accretion rate. In their model, Różanska & Czerny (2000) find $\dot{m}_{cr} \approx 0.07(\alpha_{0.1})^{3.3}$, and we adopt their result, but other models might have different \dot{m}_{cr} (see the same paper for a comparison). Due to the strong dependence on the viscosity parameter ($\alpha_{0.1} = \alpha/0.1$), one can easily get $\dot{m}_{cr} = 0.01$, without requiring unreasonable values of α ($\alpha = 0.05$ in that case). The same model predicts (for such \dot{m} and α) a discontinuous change of R_{tr} between $3R_G$ and $\sim 25R_G$. These values are slightly different from what we find (20 R_G and 50 R_G resp.), but a perfect match can hardly be expected since neither of the models producing these results could claim perfection.

4.2. Microlensing

Another reasonable possibility that could have a chance to explain the complex variability picture is a microlensing event that produces a discontinuity in the light curve. Within this explanation, the colour changes are not entirely unexpected since only a part of the disk might be magnified (Yonehara et al. 1999). The duration of the upper state (about a year) is not unreasonable as well. The microlensing model faces some difficulties, however. It is hard to explain, for instance, the change of the saturation time (Sect. 3.3). One would also expect a gradual rise and fall of the light curve, while we see quite “flat” upper state (Fig. 1). Furthermore, the colour changes have to be more gradual as the lensing body passes over different parts of the disk (the disk temperature changes gradually), but this is not the case here. Although a microlensing event cannot be entirely ruled out, all the difficulties mentioned above seem to favour the former, accretion disk structure changes possibility.

4.3. Star disruption

Star disruption near the black hole has been invoked sometimes to account for the feeding of the central engine. Recent detailed models indicate however, that such an event should be rare ($10^{-4} \div -6 \text{ yr}^{-1}$) and cannot be the primary source of accreting gas (see Ulmer 1999 for a review). Still it might, in principle, take place and eventually account for the two-state character of the light curve of Mrk 279. However, this scenario, as the previous one, encounters significant difficulties that make it unlikely:

i) The rather flat upper state is not expected. Instead, the brightness should decrease as a power law ($\propto t^{-5/3}$), as the models show.

ii) The colour changes should not be as they were observed. The brightness temperature of a standard thin disk is about 3–5000 K (assuming $F_\nu \propto \nu^{1/3}$) for the optical – near IR region, while the accreting disrupted material will have a temperature of about 10^5 K or more (Ulmer 1999). Therefore the upper state should appear relatively bluer not relatively redder in respect to the lower state, which is contrary to what the observations show.

iii) In addition to the fact that this event is found to be very rare, it is worth mentioning that the black hole of such a mass ($10^8 M_\odot$ – Sect. 1), would rather swallow a Solar type star than disrupt it, i.e. somewhat lower M_{BH} is needed for the process to be effective.

iv) Again, as in the previous case, the change of the saturation time will hardly be explained.

5. Discussion

Although none of the arguments presented in Sect. 2 alone can be convincing enough, altogether they give us confidence to conclude that the two states mentioned previously are probably real, and are not due to a small number of observations, photometric errors or just serendipity. Such a two-state variability has not been reported for the AGNs so far, however most of them have not been monitored long enough in different colours. We also note an interesting X-ray analogy, reported by Lu & Yu (1999). They find an “*Ionising luminosity – X-ray spectral index*” relation for many X-ray sources, which is remarkably similar to our optical colour–magnitude diagram (Fig. 3) built for one but variable source. Lu & Yu (1999) interpret their result in terms of the thin disk – *ADAF* paradigm, assuming that for some certain accretion rate the thin disk mode switches to an *ADAF* mode. In their work the accretion rate value, represented by the ionising luminosity, is assumed to determine the accretion regime. Similarly, we think that the best explanation for the observed two-state behaviour of Mrk 279 should be searched in a change of the transition radius (R_{tr}) between an inner *ADAF* (or any other type low-radiative solution - *CDAF*, *ADIOS*) and an outer thin disk (the radius moves inward from the lower to the higher state).

The exact variability pattern can hardly be reproduced by any simple theoretical scheme. Nonetheless, we have shown (Sect. 4) that an accretion disk structure, consisting of an inner X-ray variable *ADAF* section, and an outer thin disk with variable transition radius can reproduce the variability pattern well – both the short and the long term variations, as well as the colour changes. In order to be successful, such a scheme imposes certain restrictions on the main governing parameters – M_{BH} , \dot{m} , R_{tr} , R_{out} , α . We found that all these parameters are in a good agreement in between, according to the theoretical predictions. The assumption of a variable R_{tr} is not unusual. It is actually required for NGC 5548 as suggested by Chiang & Blaes (2003), who performed very similar modelling of the continuum of that object.

The only clear problem with the scheme we propose is that the outer thin disk has to be truncated closer to the centre than one would normally expect, i.e. at about $100R_G$. However such a small-scale disk is not necessarily irrelevant. One reason is that a thin disk is a subject of selfgravitation in its outer parts (see for details Collin & Huré 2001, Collin 2001). The selfgravitating part of the disk will eventually transform into distinct selfgravitating clouds, which if irradiated from the centre, will produce line emission rather than continuum. It has been proposed, indeed, that the selfgravitating part of a thin disk is the place where the broad lines originate. Some recent results actually suggest that the BLR should exist at a distance where an optically thick disk is already not present. Rokaki et al. (2003), for instance, find that sources pointed almost face on with respect to the observer will still reveal *broad non-shifted* emission line profiles. This fact rules out the possibility that the major part of the emission is coming from a disk or any structured flow (inflow, outflow) above an optically *thick* disk. The disk is ruled out since the profiles are too broad for a face-on orientation; the inflow/outflow is ruled out since we will not be able to see the far side of the region and the profiles will appear shifted. The only remaining possibility is a motion of clouds, with probably a flattened distribution, at a place where the disk does not extend; otherwise the clouds will strike the disk and will likely be destroyed. A good candidate for such a region is indeed the selfgravitating outer region of a thin disk. The significant breadth of the lines as well as the very broad line wings often observed suggest that such a region could start as close as $100 R_G$. Note that, if this is correct, the line width will represent mostly the vertical velocity dispersion for a face-on orientation, rather than the *Keplerian* velocity, which would lead to underestimates of the black hole masses based on the broad line velocity.

Let us consider the results from recent numerical computations for the radius at which the disk becomes selfgravitating – R_{SG} , summarised by Collin (2001). They find $R_{SG} \simeq 500R_G$ for $10^8 M_\odot$ and $\dot{m} = 0.01$, but the transition radius actually gets smaller when α is less than the canonical value of 0.1, which seems to hold here, based on the requirement $\dot{m}_{cr} \simeq 0.01$ (see Sect. 4.1). Other uncertainties, such as the exact value of the Toomre parameter Q , can also alter (and eventually further reduce) R_{SG} , making it quite close to the value we get for R_{out} .

We would also like to emphasise the connection between the *Keplerian* times at R_1 and R_2 , and the saturation times. Note that even though the brightness can change with a time interval as short as 1 day, the saturation of the variability amplitude may require a much longer time, close to τ_{var} (Sect. 3.3). It is tempting to connect the saturation time with instabilities of some sort taking place and producing variable X-ray emission at R_{tr} , and therefore being naturally associated with the dynamical timescale there. They can either be some quasi-periodic oscillations with the *Keplerian* frequency (Garcia et al. 2003), or “hot spots” of some sort originating at R_{tr} and falling inside with an almost free-fall velocity (close to the radial velocity of an *ADAF*) as described by Kawaguchi & Mineshige 1999 in their disk-

instability model. In both cases the saturation should occur at a timescale close to the dynamical one at R_{tr} .

In addition, it has to be pointed out that no stable solution providing a transition between an outer thin disk, and an inner *ADAF* has been found so far, what indirectly suggests that instabilities of some sort might occur at the transition radius, as we suggest based on our findings. Due to a scarce sampling for the object we monitored, we can estimate only the upper limit for the duration of the transition process. It is about 100 days but in fact, the real transition can be much shorter. Most probably this time should be associated with the thermal time scale of a thin disk (see Dubus 2002 for a review). Although it is not clear what triggers the transition process and switches between the regimes, it can be speculated that some small changes of accretion rate about the critical value can produce the observed picture. In fact, the estimated accretion rate of Mrk 279 is rather close to that critical value as we mentioned above. The transition between the accretion regimes, connected with a jump in accretion efficiency, can result in the dip in the brightness histogram that we observe (Fig. 2).

An ultimate test to the model we propose to account for the overall picture of variability of Mrk 297 could be provided by a hard X-ray monitoring, if such were performed. Our results suggest on average about 2-5 times higher X-ray flux during the lower *ADAF* state (for similar *V*-band magnitudes)

6. Conclusions

We describe the nature of Mrk 279’s optical variability in the following way: the long-term variations (100-300 days) are dominated by the transition between the states. These variations are probably caused by a change of the transition radius between an (inner) *ADAF* and (outer) thin disk state which is most likely due to a small change of the accretion rate around some critical value. The higher state is observed when the transition radius moves inward, increasing the area of the energetically more efficient outer thin disk. The short-term variability could be attributed to different sources. We suppose that it is connected to the processes (instabilities) that take place around the transition radius, resulting in smaller variability time-scale for the higher state.

Other explanations, like gravitational lensing or star disruption near the central black hole, can in principle also account for the observations, but these scenarios face significant difficulties to match well the variability picture. Additional EUV/X-ray data, if were available during the optical monitoring, can clarify the role of transition radius changes in cases like Mrk 279.

We summarise the results of our work in the following way:

1. Using our observational data and data from the literature, we build seven-years optical *BVRI* light curve of the Seyfert 1 type galaxy Mrk 279. The typical errors of the photometry are about 0^m02.

2. Analysing the data we find arguments in favour of the possibility that Mrk 279 shows different states of brightness. They are characterised by different colour-magnitude relations and different short-term variability.
3. We find that these states may result from a transition between the thin disk and the *ADAF* accretion modes, as our modelling shows. This hypothesis does not confront the observational data.

Finally, we would like to emphasise that such regular multicolour observations, even performed with the facilities of smaller observatories, can bring important information about the AGN variability. The physics of accretion flows is not yet well understood, and we think that such observations might help when the processes, taking place at the AGN centres, are modelled.

Acknowledgements. CCD ST-8 at the Observatory of Belogradchik is provided by Alexander von Humboldt foundation, Germany. Skinakas Observatory is a collaborate project of the University of Crete, the Foundation for Research and Technology - Hellas, and the Max-Planck-Institut für Extraterrestrische Physik. The authors are grateful to Dr. Becky Grouchy for some technical help, as well as to our anonymous referee for his/her criticism that helped to improve much this paper.

References

- Bachev, R., Strigachev, A., Petrov, G.T., et al.: 1999, Bulgarian Journal of Physics 5/6, 1
- Bachev, R., Strigachev, A., Dimitrov, V.: 2000, A&AS 147, 175
- Bian, W., Zhao Y.: 2003, PASJ 55, 143
- Chiang, J., Blaes, O.: 2003, ApJ 586, 97
- Collier, S., Peterson, B.M.: 2001, ApJ 555, 775
- Collin, S., in "Advanced Lectures on the Starburst-AGN Connection", Puebla Mexico, World Scientific: 2001, p.167
- Collin, S., Huré, J.-M.: 2001, A&A 371, 50
- di Clemente, A., Giallongo, E., Natali, G., et al.: 1996, ApJ 463, 466
- Dubus, C.: 2002, astro-ph/0206218
- Esin, A.A., McClintock, J.E., Narayan R.: 1997, ApJ 489, 865
- Frank, J., King, A., Raine, D.: 2002, "Accretion Power in Astrophysics", Cambridge University
- Garcia, J., Peitz, J., Keller, C. et al.: 2003, astro-ph/0301113
- Ho, L.C.: 1998, in "Observational Evidence for Black Holes in the Universe", Kluwer, Ed. S.K. Chakrabarti
- Kawaguchi, T., Mineshige, S., Umemura, M., et al.: 1998, ApJ 504, 671
- Kawaguchi, T., Mineshige, S.: 1999, in "Active Galactic Nuclei and Related Phenomena", IAUS 194, p.356
- Lu, Y., Yu, Q.: 1999, ApJ 526, L5
- Maoz, D., Netzer, H., Leibowitz, E., et al.: 1990, ApJ 351, 75
- Narayan, R., Mahadevan, R., Quataert, E.: 1998, in "Theory of Black Hole Accretion Discs", Eds. M.A. Abramowicz, G. Bjornsson and J.E. Pringle, Cambridge, p.148
- Rokaki, E., Lawrence, A., Economou, F. et al.: 2003, astro-ph/0301405
- Rózanska, A., Czerny, B.: 2000, A&A 360, 1170
- Santos-Lleo, M., Clavel, J., Schulz, B., et al.: 2001, astro-ph/0102356
- Stirpe, J.: 1991, in "Variability of Active Galaxies", Eds. W.J. Duschl, S.J. Wagner, M. Camenzind, Springer-Verlag, p.71.
- Ulmer, A.: 1999, ApJ 514, 180
- Ulrich, M.-H., Maraschi, L., Urri, M.C.: 1997, ARA&A 35, 445
- Yonehara, A., Mineshige, S., Fukue, J. et al.: 1999, A&A 343, 41

Appendix A: Table and figures

Table A1. Magnitudes of Mrk 279 (our observations only)

JD (2450000+)	B	V	R	I
634.4	14.6	14.09	13.52	13.15
640.5	14.6	14.05	13.50	13.12
661.4	14.5	14.04	13.46	13.08
664.4	14.4	14.03	13.45	13.05
665.4	14.5	14.04	13.45	13.07
666.5	14.5	14.00	13.45	13.07
668.4	14.6	14.01	13.44	13.06
669.4	14.5	14.03	13.44	13.06
721.3	14.5	14.08	13.51	13.13
844.6	14.2	13.78	13.31	12.96
875.6	14.1	13.70	13.24	12.90
930.4	14.3	13.85	13.32	12.94
931.5	14.4	13.86	13.32	12.94
962.5	14.2	13.81	13.29	12.90
964.5	14.3	13.79	13.24	12.88
965.5	14.3	13.77	13.24	12.87
981.5	14.2	13.73	13.25	12.89
1012.3	14.3	13.73	13.25	12.89
1013.3	14.3	13.73	13.24	12.87
1014.3	14.3	13.81	13.29	12.92
1015.3	14.3	13.85	13.29	12.92
1016.3	14.3	13.84	13.31	12.92
1017.3	14.3	13.86	13.30	12.92
1050.5	14.4	13.83	13.28	12.92
1052.3	14.2	13.80	13.29	12.91
1083.4	14.3	13.80	13.26	12.90
1085.3	14.2	13.80	13.29	12.92
1201.5	14.8	14.15	13.53	13.11
1226.5	14.6	14.11	13.53	13.11
1252.6	14.5	14.00	13.47	13.08
1258.5	14.4	13.99	13.46	13.08
1288.5	14.4	13.95	13.42	13.05
1289.4	14.4	13.94	13.41	13.04
1344.4	14.6	14.17	13.56	13.16
1366.4	14.5	14.05	13.50	13.12
1367.3	14.7	14.11	13.48	13.10
1409.3	14.4	13.98	13.44	13.05
1410.4	14.4	13.97	13.41	13.05

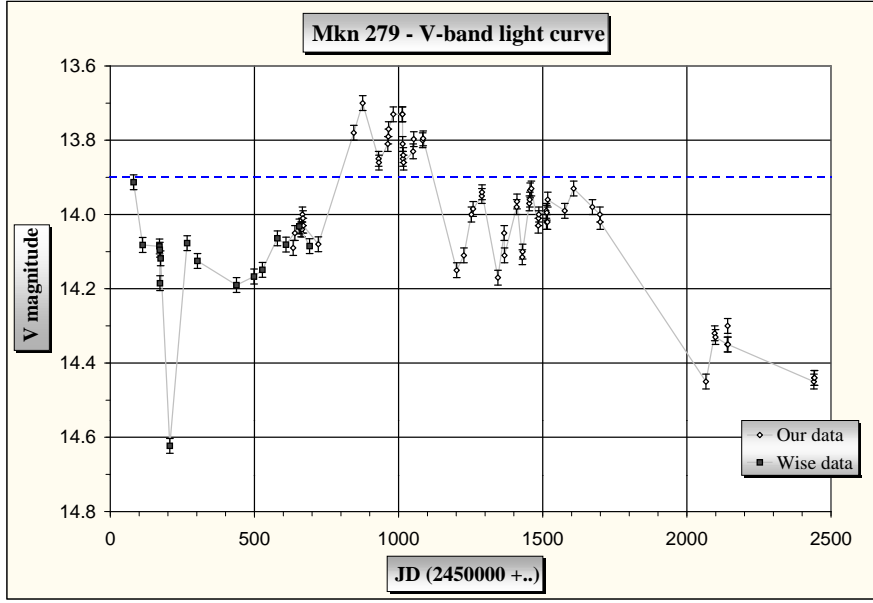


Fig. A1. V-band light curve of Mrk 279. Magnitudes are measured in 16'' diaphragm. The filled squares are Wise Observatory magnitudes and the rombs are our data. The dashed line represents a possible division between two different states (see also Fig. 3).

Table A1. *continued*

JD (2450000+)	B	V	R	I
1429.3	14.7	14.12	13.54	13.15
1430.3	14.6	14.10	13.53	13.14
1453.2	14.6	13.97	13.43	13.03
1455.3	14.4	13.96	13.42	13.04
1456.3	14.5	13.94	13.42	13.05
1460.2	14.4	13.93	13.40	13.02
1484.3	14.5	14.03	13.46	13.09
1485.2	14.5	14.01	13.47	13.06
1486.2	14.5	14.00	13.44	13.05
1512.2	14.5	13.99	13.44	13.06
1513.2	14.6	14.02	13.47	13.07
1514.2	14.4	14.00	13.43	13.05
1516.2	14.6	14.02	13.46	13.07
1517.2	14.5	13.96	—	—
1576.6	14.5	13.99	13.46	13.09
1607.5	14.4	13.93	13.42	13.04
1672.5	14.5	13.98	13.44	13.07
1698.3	14.5	14.00	13.45	13.07
1699.3	14.5	14.02	13.47	13.09
2066.3	—	14.45	13.93	13.39
2096.3	—	14.32	13.78	—
2099.3	—	14.33	13.78	13.31
2140.4	14.9	14.35	13.73	13.31
2141.4	14.7	14.30	13.68	13.25
2142.4	14.6	14.35	13.70	13.29
2440.4	15.0	14.45	13.85	13.38
2441.4	14.9	14.44	13.83	13.36
2442.4	15.0	14.44	13.81	13.36

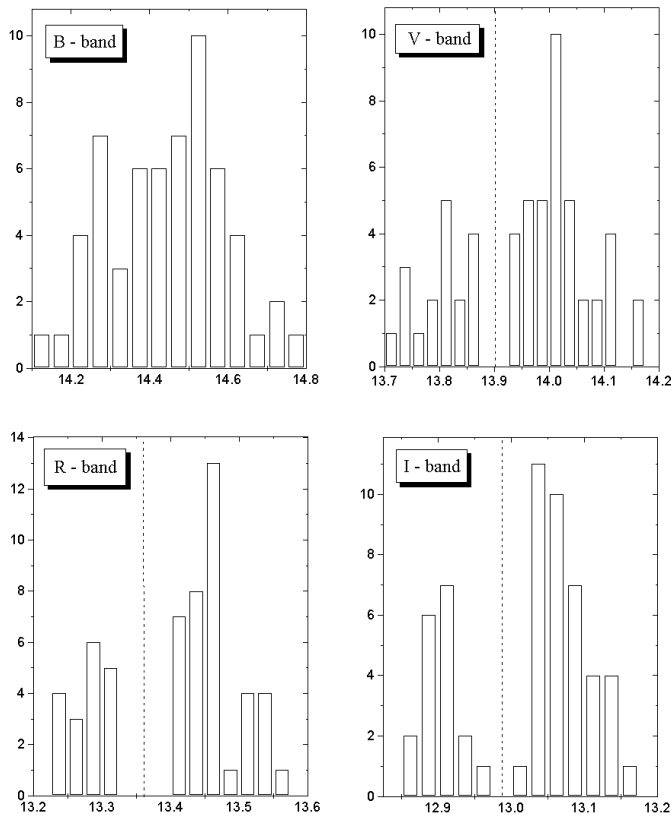


Fig. A2. Brightness histograms for B , V , R and I -bands respectively. The bimodal distribution is clearly seen (except for B -band). The histograms are based on both – our data and the Wise Observatory data. A few observational points where the object was very faint are not used.

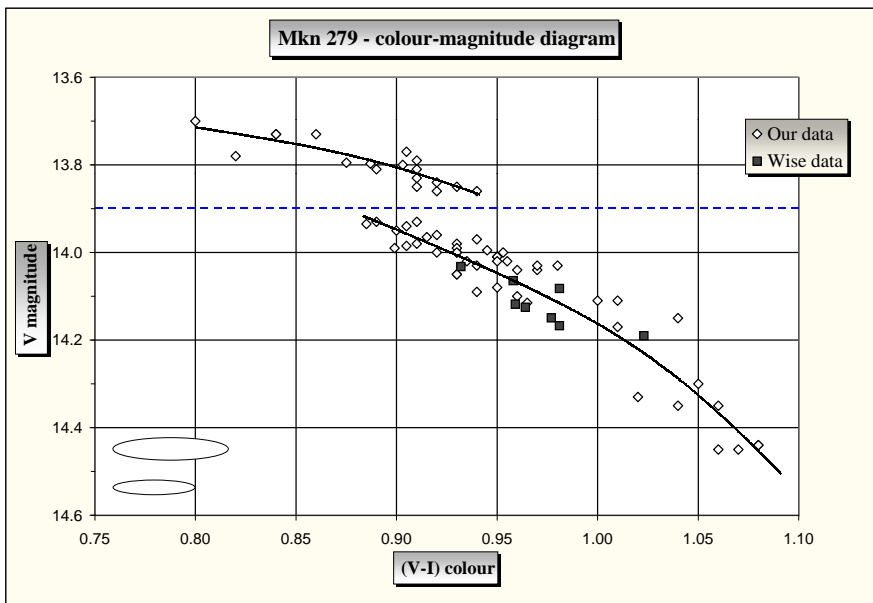


Fig. A3. The relation between the colour ($V - I$) and the V -band magnitudes of Mrk 279. A jump in the relation is clearly seen. The thick lines are to guide the eye. The filled squares are the Wise Observatory magnitudes and the rombs are the our data. The dashed line shows the division between the two states. The large ellipse at the lower left corner of the picture indicates the area that contains about 67% of all V vs. $V - I$ points for the check star, measured in respect to the main standard. As such, it is an estimate of the photometric errors. The smaller ellipse is a similar prediction for the variable AGN, taking into account the much better statistics we get for it. It is seen that the two-state behaviour is highly unlikely to be due to photometric errors.

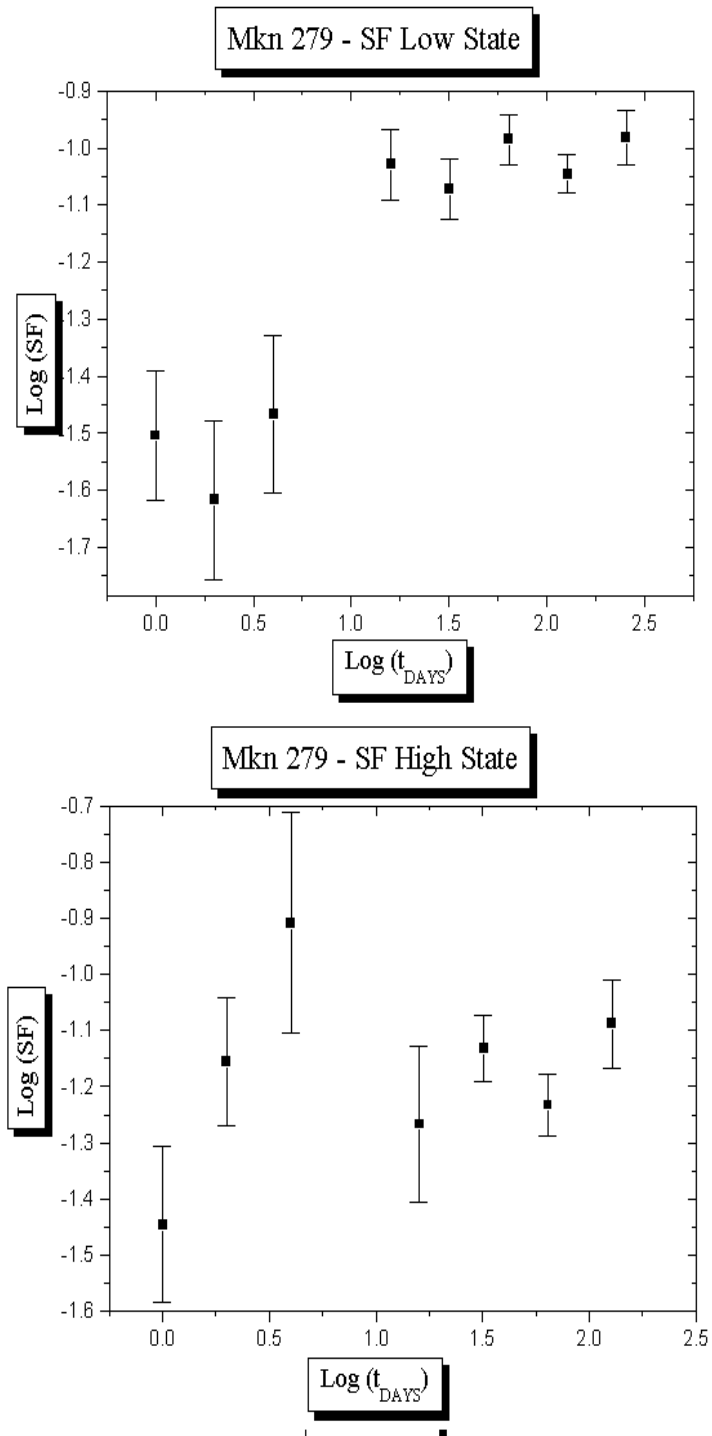


Fig. A4. The SF s for the upper state (based on 18 points) and the lower state (based on 30 points, starting immediately after the high state). It is important to note that the saturation time scale is very short, in order of several days. Furthermore this time is different for the lower and the higher states – resp. 20 and 3-5 days.

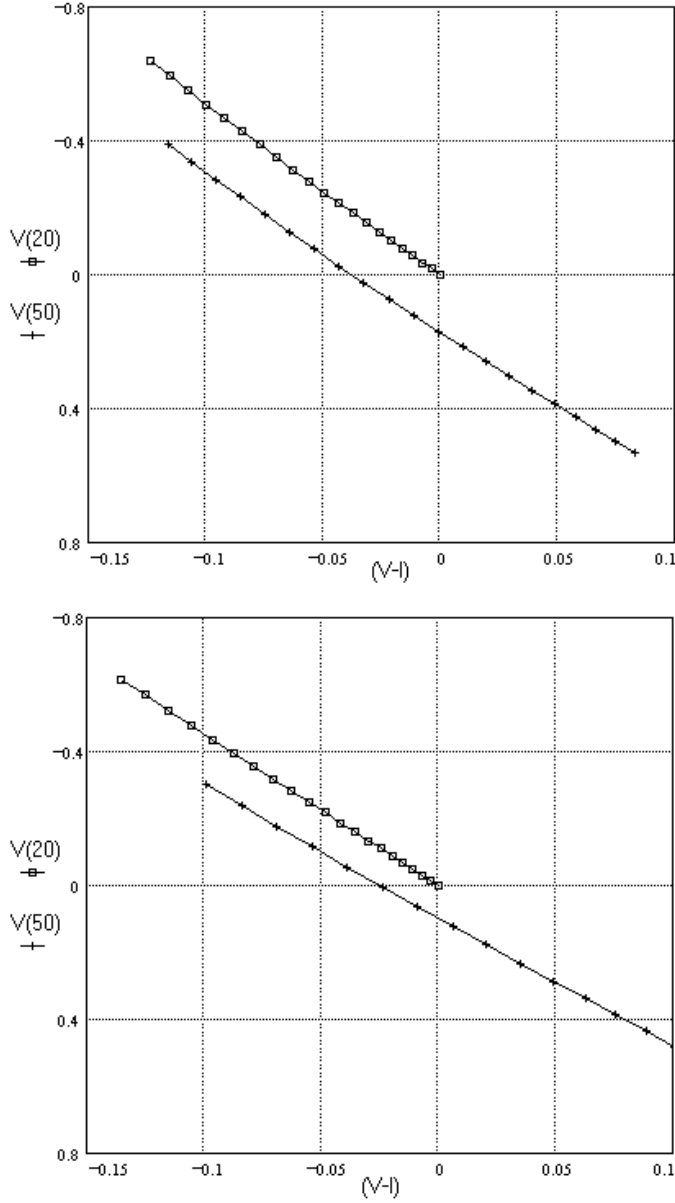


Fig. A5. Results from the continuum variations modelling – $(V - I)$ colour vs. V -magnitude (relative units used). Here $\dot{m} = 0.01$, $R_{out} = 100R_G$ and L_x is a free parameter, which changes produce the short-term optical variability (the thick lines). Each point along the curves represents a change of $\log(L_x)$ by 0.05, the full range of change of L_x is the same for both curves. The two curves shown are for different $R_{tr} = 20$ (the upper one) and 50 (the lower one) R_G . The upper picture is for a black hole mass $\log(M_{BH}) = 7.5$, the lower one – $\log(M_{BH}) = 8$. These two solutions are found to mimic best the true variability picture (Fig. 3).